THE JOURNAL OF PHYSICAL CHEMISTRY A

Article

Cite This: J. Phys. Chem. A XXXX, XXX, XXX−XXX

pubs.acs.org/JPCA

A Multireference Ab Initio Study of the Diradical Isomers of Pyrazine

Published as part of The Journal of Physical Chemistry virtual special issue "Hanna Reisler Festschrift".

Thais Scott,[†,∥] Reed Nieman,[‡] Adam Luxon,[†] Boyi Zhang,[†] Hans Lischka,[‡,§] Laura Gagliardi,[∥] and Carol A. Parish*[,†]

[†]Department of Chemistry, Gottwald Center for the Sciences, University of Richmond, Richmond Virginia 23713, United States

[‡]Department of Chemistry and Biochemistry, Texas Tech University, Lubbock, Texas 79409-1061, United States

[§]School of Pharmaceutical Sciences and Technology, Tianjin University, Tianjin, 300072 P.R. China

[∥]Department of Chemistry, Chemical Theory Center and the Minnesota Supercomputing Institute, The University of Minnesota, Minneapolis, Minnesota 55455, United States

Supporting Information

ABSTRACT: Three diradical pyrazine isomers were characterized using highly correlated, multireference methods. The lowest lying singlet and triplet state geometries of 2,3-didehydropyrazine (*ortho*), 2,5-didehydropyrazine (*para*), and 2,6-didehydropyrazine (*meta*) were determined. Two active reference spaces were utilized. The complete active space (CAS) (8,8) includes the σ and σ^* orbitals on the dehydrocarbon atoms as well as the valence π and π^* orbitals. The CAS (12,10) reference space includes two additional orbitals corresponding to the in-phase and out-of-phase nitrogen lone pair orbitals. Adiabatic and vertical gaps between the lowest lying singlet and triplet states, optimized geometries, canonicalized orbital energies, unpaired electron densities, and spin polarization effects were compared. We find that the singlet states of each diradical isomer contain two significantly weighted configurations, and the larger active space is necessary for the proper physical characterization of both the singlet and triplet states. The singlet−triplet splitting is very small for the 2,3-didehydropyrazine (*ortho*) and 2,6-didehydropyrazine (*meta*) isomers (+1.8 and −1.4 kcal/mol, respectively) and significant for the 2,5-didehydropyrazine (*para*) isomer (+28.2 kcal/mol). Singlet geometries show through-space interactions between the dehydrocarbon atoms in the 2,3-didehydropyrazine (*ortho*) and 2,6-didehydropyrazine (*meta*) isomers. An analysis of the effectively unpaired electrons suggests that the 2,5-didehydropyrazine (*para*) isomer also displays through-bond coupling between the diradical electrons.

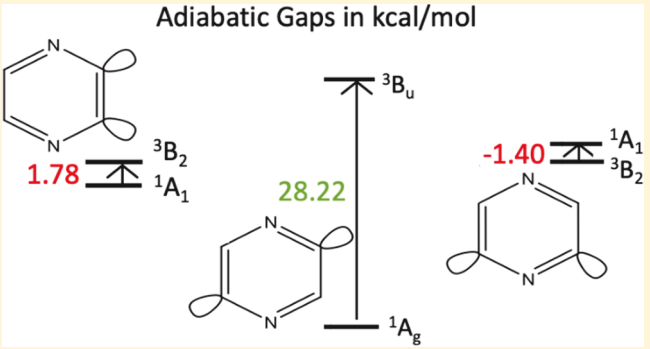

INTRODUCTION

Molecules containing more than one unpaired electron are difficult to study using either experimental or computational methods. Experimentally, the high reactivity and fleeting existence of di- and polyradicals makes these species difficult to isolate and characterize. Their complicated electronic structure is difficult to describe accurately. Exploring the structure and energetics of diradicals is an important step to improving the effectiveness of antitumor drugs and understanding certain bond making and breaking processes in organic syntheses. Anticancer drugs, such as dynemicin,[1] esperamicin,[2] and calicheamicin[3] use diradicals to deprotonate DNA, leading to cell death. The deprotonation of DNA is predicted to occur when the diradical is in the lowest lying triplet state as it is in this state where the radical electrons are less coupled. However, through-bond or through-space coupling may lead to singlet ground states.[4] Therefore, knowledge of the electron configuration of the ground state as well as the singlet−triplet energy gap is critical in understanding the behavior of a diradical.[4] It is also the case that diradical hydrogen abstraction is nonspecific and targets the DNA of both healthy and cancerous cells. Traditionally, natural product-based diradicals contained benzyne; however, tunable structures are necessary for improving future drug design and the pyrazine analogs of benzyne have been suggested as a potential modification for use in novel anticancer agents.[5] Additionally, heteroarynes containing nitrogen are often intermediates in synthetic organic and inorganic chemistry. For instance, it has been shown experimentally that 2,3-didehydropyrazine is an intermediate in the elimination of hydrochloric acid from chloropyrazine by iron[6] and is thought to be an intermediate in the pyrolysis of pyrazine-2,3-dicarboxylic acid anhydride.[7] This study will focus on the characterization of 2,3-didehydropyrazine (*ortho*), 2,5-

Received: December 26, 2018
Revised: February 15, 2019
Published: February 19, 2019

DOI: 10.1021/acs.jpca.8b12440
J. Phys. Chem. A XXXX, XXX, XXX−XXX

didehydropyrazine (*para*), and 2,6-didehydropyrazine (*meta*) diradical isomers (Figure 1).

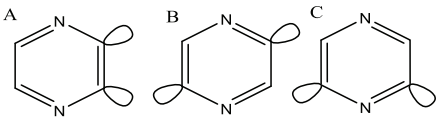

Figure 1. (A) 2,3-Didehydropyrazine (*meta*), (B) 2,5-didehydropyrazine (*para*), and (C) 2,6-didehydropyrazine (*ortho*). Lobes represent the positions of the radical electrons.

Previous to the work reported here, the most thorough theoretical study on diradical pyrazines was reported in 2003 by Cioslowski in a wide-ranging study that characterized many heterocyclic diradicals.[8] The Cioslowski study was restricted to single reference wave functions to characterize these systems; however, the diradical isomers of pyrazine are likely multireference in the singlet state.[4,9] It has been shown that the diradical isomers of benzene require a multiconfigurational reference function to accurately describe the singlet−triplet gap.[10−18] To the best of our knowledge, these diradical forms of pyrazine have not been studied previously using either experimental or multireference theoretical methods. To allow for the possibility that diradical pyrazines are multiconfigurational in nature, highly correlated multireference methods were used in this study to determine the geometry of the lowest lying singlet and triplet state as well as to evaluate the singlet−triplet splitting in the diradical pyrazine isomers.

We pursued the proper physical characterization of these species using a variety of state-of-the-art *ab initio* methods. First, we utilized complete active space self-consistent field theory (CASSCF) to generate multireference wave functions, which accounted for static correlation. We then applied multireference configuration interaction with single and double excitations (MR-CISD) and multireference averaged quadratic coupled cluster (MR-AQCC) theory to obtain accurate reference benchmarks. We considered the MR-AQCC results as our primary benchmark, as this method has been shown previously to properly characterize the biradicaloid character of compounds such as acenes,[19] heptazethrene,[20] and nitrogen-doped derivatives thereof as well as the biradical character of *p*-benzyne.[21,22] MR-AQCC provides a well-balanced description of quasi-degenerate orbital effects and allows also for the efficient inclusion of dynamic electron correlation. For comparison purposes, we also utilized a popular, relatively efficient second-order perturbative method, complete active space perturbation theory through second order (CASPT2). Lastly, we applied the multiconfigurational pair density functional theory (MC-PDFT) to the diradical isomer characterizations. MC-PDFT is a recently developed DFT-based method that has been shown to produce results with oligoacenes that are highly accurate at a fraction of the computational cost of higher-level methods.[23] These methods were used to more accurately describe electron correlation. With these methods, the geometries and singlet triplet energies of these isomers can be accurately determined. From this, we will be able to determine the most effective pyrazine-based alternative to current diradical antitumor warheads.

COMPUTATIONAL METHODS

The triplet state of each isomer was used to obtain initial molecular orbitals and geometries. This preliminary calculation was performed using the single reference restricted open shell Hartree−Fock (ROHF) method with the cc-pVDZ basis set as implemented in the Gaussian 09 software.[24] The molecular orbitals were assigned irreducible representations using the C_{2v} point group for the *ortho* (2,3) and *meta* (2,6) isomers and C_{2h} for the *para* (2,5) isomer. All calculations described below were performed with both the cc-pVDZ and cc-pVTZ basis sets[25,26] of Dunning and co-workers to explore the effect of basis set size.

A complete active space (CAS) of 8 electrons and 8 orbitals was used to optimize a reference wave function for each isomer. The orbitals in the CAS (8,8) included the σ and σ^* orbitals on the dehydrocarbon atoms and the π and π^* orbitals, depicted in Table 1A. A CAS (12,10) active space was also utilized to probe the interaction of the radical electrons with the lone pair orbitals on the nitrogen atoms. For each isomer the expanded active space included the in-phase and out-of-phase orbitals corresponding to the lone pair electrons of the

Table 1. (A) CAS (8,8) Orbitals Ordered by the Energies of the MCSCF Canonicalized Orbitals for the *Ortho* (2,3) (C_{2v}), *Meta* (2,6) (C_{2v}), and *Para* (2,5) (C_{2h}) Diradical Isomers of Pyrazine; (B) in-Phase and out-of-Phase Combinations of Lone Pair Orbitals from the Nitrogen Atoms Added To Form the CAS (12,10) Active Space

1A

ortho (2,3)	*para* (2,5)	*meta* (2,6)
π_1 ($1b_1$)	π_1 ($1a_u$)	π_1 ($1b_1$)
π_2 ($1a_2$)	π_2 ($1b_g$)	π_2 ($2b_1$)
π_3 ($2b_1$)	π_3 ($2b_g$)	π_3 ($1a_2$)
σ ($10a_1$)	σ^* ($9b_u$)	σ ($11a_1$)
σ^* ($8b_2$)	σ ($9a_g$)	σ^* ($7b_2$)
π_4^*($3b_1$)	π_4^* ($2a_u$)	π_4^*($3b_1$)
π_5^* ($2a_2$)	π_5^*($3a_u$)	π_5^*($2a_2$)
π_6^* ($3a_2$)	π_6^* ($3b_g$)	π_6^* ($4b_1$)

1B

ortho (2,3)	*para* (2,5)	*meta* (2,6)
$9a_1$	$8a_g$	$10a_1$
$7b_2$	$8b_u$	$9a_1$

DOI: 10.1021/acs.jpca.8b12440
J. Phys. Chem. A XXXX, XXX, XXX−XXX

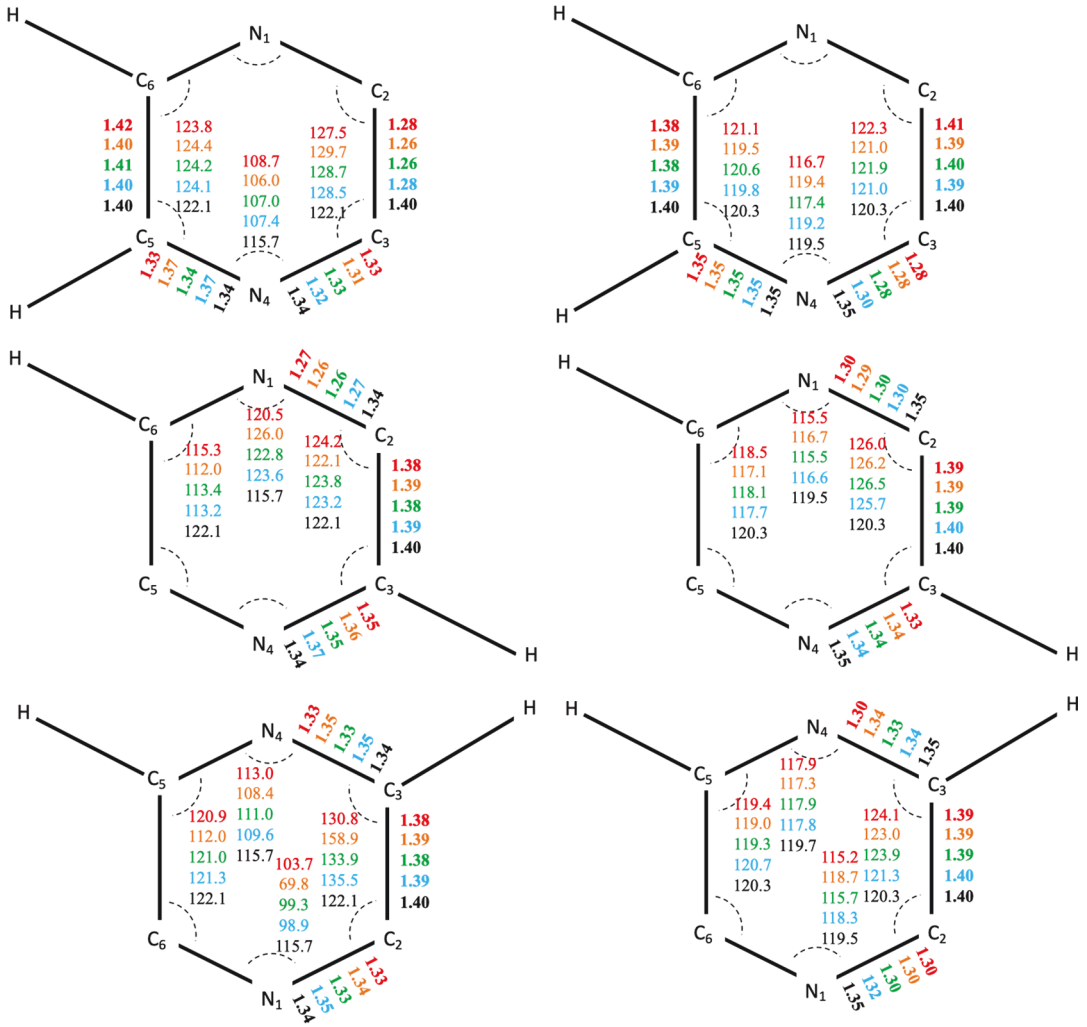

Figure 2. Optimized singlet (left) and triplet (right) geometries for each isomer obtained using (8,8) CASSCF (red), MR-CISD (green), MR-AQCC (blue), and (12,10) MC-PDFT (orange), with the cc-pVTZ basis set. The bold text outside of the ring are the bond distances (Å). Bond angles (degrees) are shown inside the ring. Top row: *ortho* (2,3) isomer. Middle row: *para* (2,5) isomer. Bottom row: *meta* (2,6) isomer. For comparison, the geometries of the lowest lying singlet and triplet states of fully saturated pyrazine are included on each image (black). These values for fully saturated pyrazine were obtained from electron diffraction (singlet)[45] and CCSDR(3)/def2-TZVPP calculations (triplet).[46]

nitrogen atoms. These additional orbitals are shown in Table 1B.

The two states that were investigated for each isomer were the lowest lying triplet and singlet states. Each of these states has been calculated independent of the other. For *ortho* (2,3) and *meta* (2,6) the lowest lying singlet and triplet states correspond to the $^1A_1$ and $^3B_2$ electronic states and for *para* (2,5) the lowest lying singlet state was ^1A_g and the lowest lying triplet was ^3B_u.

We utilized CASSCF[27] to generate configuration state functions (CSFs) by dividing the orbital space into doubly occupied orbitals (DOCC), the complete active space orbitals (CAS), and the virtual orbitals. To account for static and dynamic electron correlation, we used multireference configuration interaction with singles and doubles (MR-CISD) as well as a multireference-quadratic coupled cluster (MR-AQCC) method. These methods have recently been reviewed.[28,29] It is important to note that analytical energy gradients are available for these highly correlated methods.[30] The MR-CISD[31] and MR-AQCC[32] calculations utilized a frozen core containing the lowest lying orbitals in each isomer (*ortho* (2,3) $1b_2$, $1a_1$, $2a_1$, $2b_2$, $3a_1$, $3b_2$; *para* (2,5) $1b_u$, $2a_g$, $2b_u$, $2a_g$, $3b_u$, $3a_g$; *meta* (2,6) $1a_1$, $2a_1$, $3a_1$, $1b_2$, $2b_2$, $4a_1$). All other occupied orbitals not contained in the CAS were a part of the DOCC and were doubly occupied in all reference configurations. Excitations out of these DOCC orbitals are considered in the final CSF expansion as well. The geometries and wave functions generated from the CASSCF calculations were used as input for the MR-CISD calculations. Additionally, the optimized geometries generated from the MR-CISD calculations were used as input for the MR-AQCC calculations. We also employed MC-PDFT[33,34] to optimize the geometries and compute the electronic energy differences of the various isomers. In MC-PDFT a multireference wave function is used to compute the kinetic energy and the classical coulomb energy. The density and on-top pair density obtained from the multireference wave function are then employed to compute the remaining energy terms using an on-top density functional. In our case we used CASSCF multireference wave functions as described above. The MC-PDFT geometry optimizations were performed using the newly developed MC-PDFT analytical gradients.[35] The MC-PDFT calculations were performed using *OpenMolcas* in the Molcas 8.0

DOI: 10.1021/acs.jpca.8b12440
J. Phys. Chem. A XXXX, XXX, XXX−XXX

Table 2. CASSCF, MR-CISD, MR-CISD+Q, and MR-AQCC Adiabatic Excitation Energies (kcal/mol) from the Ground State Using a CAS (8,8) Reference Wave Function and the cc-pVTZ Basis Set

isomer	state	dominant configuration in MR-AQCC[c]	CASSCF[a]	MR-CISD[a]	MR-CISD+Q[a]	MR-AQCC[a]
ortho (2,3)	$^1A_1$	57.0% $\pi_1^2\pi_2^2\pi_3^2\sigma^2$ + 8.3% $\pi_1^2\pi_2^2\pi_3^2\sigma^{*2}$				
	$^3B_2$	58.1% $\pi_1^2\pi_2^2\pi_3^2\sigma^{*1}\sigma^1$ + 9.5% $(9a_1)^1\pi_1^2\pi_2^2\pi_3^2\sigma^2\sigma^{*1}$	8.88	7.89	6.03	−0.89
para (2,5)	^1A_g	58.1% $\pi_1^2\pi_2^2\pi_3^2(\sigma^*)^2$ + 7.5%$\pi_1^2\pi_2^2\pi_3^2\sigma^2$				
	^3B_u	66.0% $\pi_1^2\pi_2^2\pi_3^2\sigma^{*1}\sigma^1$ + 2.2% $(8a_g)^1\pi_1^2\pi_2^2\pi_3^2\sigma^2\sigma^{*1}$	11.57	19.45	25.82	25.32[b]
meta (2,6)	$^1A_1$	57.5% $\pi_1^2\pi_2^2\ \pi_3^2\ \sigma^2$ + 10.8% $\pi_1^2\pi_2^2\pi_3^2(\sigma^*)^2$				
	$^3B_2$	57.0% $\pi_1^2\pi_2^2\pi_3^2\sigma^{*1}\sigma^1$ + 6.8% $(10a_1)^1\pi_1^2\pi_2^2\pi_3^2\sigma^2\sigma^{*1}$	1.93	2.02	2.27	−6.04[b]

[a]All absolute energies are reported in the Supporting Information in Table S7. [b]Intruder state has been added to the reference space at the MR-AQCC level. Details are included in the Computational Methods. [c]Percent weights correspond to the square of the coefficients of each configuration, i.e., (c^2*100)

program.[36] The CASSCF energies computed with *OpenMolcas* and COLUMBUS differ by less than 0.005 kcal/mol.

The parallel COLUMBUS package[37−40] was used to perform geometry optimization, single point, orbital energy, and effective unpaired electron density calculations at the CASSCF (8,8), MR-CISD (8,8), and MR-AQCC (8,8) levels of theory. In addition, COLUMBUS was used to perform MR-AQCC (12,10)/cc-pVTZ single point energy calculations on the MR-AQCC (8,8)/cc-pVTZ geometries. The Molcas 8.0 program[36] was used to perform the CASPT2 and MC-PDFT geometry optimizations and single point calculations. Geometry optimizations using CAS (12,10) were not possible at the MR-CISD and MR-AQCC levels of theory with current computational resources. Zero-point energy corrections were not included.

Initially, the MR-AQCC (8,8) geometry optimization for the *para* (2,5) isomer singlet state did not converge due to an intruder state that consisted of a single excitation from the DOCC $8a_g$ orbital, corresponding to the in-phase combination of lone pair electrons on the nitrogen atoms, to the CAS $9a_g$ orbital. Such CSFs not contained in the reference space with a significant weight of more than 1% (3% for 2,3 ortho triplet) were considered to be intruder states and were individually added to the reference configuration space. This modified CAS (8,8) active space augmented by the individual intruder state configuration was utilized to generate the energies and optimized geometries for the *para* (2,5) isomer singlet state at the MR-AQCC level of theory. The additional reference configuration was not included in the calculation of the triplet state of the *para* (2,5) isomer due to symmetry considerations. An intruder state also prevented the geometry of the singlet state of the *meta* (2,6) isomer from converging in our initial calculations. This intruder state involved excitation from the DOCC $10a_1$ orbital to the CAS $11a_1$ orbital and was manually included in the same manner as detailed above.

In the results below, we report singlet−triplet energy gaps as $E(ST)$ = (triplet − singlet); therefore, a positive $E(ST)$ indicates that the singlet lies lower in energy than the triplet. To obtain vertical excitations that may prove useful for spectroscopists, single-point computations of the triplet state were performed at the CASSCF (8,8), MR-CISD (8,8), and MR-AQCC (8,8) levels of theory on the singlet geometry for each isomer. Canonicalized orbital energies were calculated at the CASSCF/cc-pVTZ level of theory. MR-AQCC (12,10)/cc-pVTZ unpaired electron density (UED) was generated for the lowest-lying singlet and triplet states of all isomers, using the COLUMBUS software. A table depicting the calculations performed with each active space is shown below.

The number of effectively unpaired electrons (N_U) was calculated using

$$N_U = \sum_{i=1}^{M} n_i^2(2 - n_i)^2$$

where M is the total number of natural orbitals used and n_i is the occupation number of natural orbital i. This is the nonlinear definition of unpaired electrons from Head-Gordon.[41] We chose this approach as it reduces the importance of contributions from nearly doubly occupied or nearly unoccupied natural orbitals (NOs) relative to the linear function. Orbital representations and UED visualizations were generated with Molden,[42] Jmol,[43] and Visual Molecular Dynamics.[44] In the results presented below we highlight the cc-pVTZ results. Calculations performed with the cc-pVDZ basis set on all isomers can be found in the Supporting Information in Tables S2, S3, S5 and S8.

RESULTS AND DISCUSSION

Optimized Geometries. The diradical geometries calculated using CASSCF (8,8), MR-CISD (8,8), MR-AQCC (8,8), and MC-PDFT (12,10) are presented in Figure 2. Our most accurate geometries were obtained at the MR-AQCC (8,8)/cc-pVTZ level as it is in this method that the wave function has the most accurately described dynamical correlation. For comparison purposes, we also include in Figure 2 the geometry for the fully saturated singlet state determined using gas-phase electron diffraction[45] and the fully saturated triplet state determined using the CCSDR(3)/def2-TZVPP method.[46]

The *ortho* (2,3) pyrazine singlet shows two significant distortions from the saturated pyrazine geometry. The C_2-C_3 bond is shortened by 0.12 Å, and the $C_3-N_4-C_5/C_2-N_1-C_6$ angle is 8.3° smaller. The shortened C_2-C_3 bond is an expected result as it has been shown that radical electrons on neighboring carbon atoms form bond-like interactions in the singlet state.[47] It is notable that in a previous report QCISD/cc-pVDZ failed to converge on a geometry for the singlet state of *ortho* (2,3) didehydroprazine.[8] The *ortho* (2,3) triplet state contains a dehydrocarbon−nitrogen (N_4-C_3/N_1-C_2) bond that is 0.05 shorter than in the saturated pyrazine triplet. Otherwise, the bond lengths and angles in the triplet state do not show much distortion from saturated pyrazine; with a difference of at most 0.01 Å or 0.7°. In the triplet state of this isomer, there is little methodological dependence in the structure.

In the singlet state of the *para* (2,5) isomer, there are three major distortions. The N_1-C_2 bond is shorter than in fully saturated pyrazine by 0.07 Å. The bond shortening is similar to

DOI: 10.1021/acs.jpca.8b12440
J. Phys. Chem. A XXXX, XXX, XXX−XXX

Table 3. CASSCF, MR-CISD, MR-CISD+Q, and MR-AQCC Vertical Excitation Energies (kcal/mol) from the Ground State Using CAS (8,8) Reference Wave Function and the cc-pVTZ Basis Set[a]

isomer	state	dominant configuration in MR-AQCC	CASSCF	MR-CISD	MR-CISD+Q	MR-AQCC
ortho (2,3)	$^1A_1$	57.0% $\pi_1^2\pi_2^2\pi_3^2\sigma^2$ + 8.3% $\pi_1^2\pi_2^2\pi_3^2\sigma^{*2}$				
	$^3B_2$	58.1% $\pi_1^2\pi_2^2\pi_3^2\sigma^{*1}\sigma^1$ + 9.5% $(9a_1)^1\pi_1^2\pi_2^2\pi_3^2\sigma^2\sigma^{*1}$	25.33	23.09	20.70	15.30
para (2,5)	^1A_g	58.0% $\pi_1^2\pi_2^2\pi_3^2(\sigma^*)^2$ + 7.5% $\pi_1^2\pi_2^2\pi_3^2\sigma^2$				
	^3B_u	66.0% $\pi_1^2\pi_2^2\pi_3^2\sigma^{*1}\sigma^1$ + 2.2% $(8a_g)^1\pi_1^2\pi_2^2\pi_3^2\sigma^2\sigma^{*1}$	18.22	26.21	31.57	30.92
meta (2,6)	$^1A_1$	57.5% $\pi_1^2\ \pi_2^2\pi_3^2\sigma^2$ + 10.8% $\pi_1^2\pi_2^2\pi_3^2\ (\sigma^*)^2$				
	$^3B_2$	57.0% $\pi_1^2\pi_2^2\pi_3^2\sigma^{*1}\sigma^1$ + 6.8% $(10a_1)^1\pi_1^2\pi_2^2\pi_3^2\sigma^2\sigma^{*1}$	12.26	18.76	13.07	5.48

[a]All absolute energies are reported in the Supporting Information in Table S7.

Table 4. MR-AQCC Adiabatic Excitation Energies (kcal/mol) from the Ground State Using CAS (8,8) and CAS (12,10) Reference Wave Functions and the cc-pVTZ Basis Set at the MR-AQCC (8,8) Optimized Geometry

isomer	state	dominant configuration in MR-AQCC (12,10)	MR-AQCC (12,10)[a]	dominant configuration in MR-AQCC (8,8)	MR-AQCC (8,8)[a]
ortho (2,3)	$^1A_1$	58.8% $\pi_1^2\pi_2^2\pi_3^2\ \sigma^2$ + 7.7% $\pi_1^2\pi_2^2\pi_3^2\ (\sigma^*)^2$		57.0% $\pi_1^2\pi_2^2\pi_3^2\ \sigma^2$ + 8.3% $\pi_1^2\pi_2^2\pi_3^2\ \sigma^{*2}$	
	$^3B_2$	64.2% $\pi_1^2\pi_2^2\pi_3^2(\sigma^*)^1\sigma^1$	1.78	58.6% $\pi_1^2\pi_2^2\pi_3^2\sigma^{*1}\sigma^1$ + 9.5% $(9a_1)^1\pi_1^2\pi_2^2\pi_3^2\sigma^2\sigma^{*1}$	−0.89
para (2,5)	^1A_g	56.5% $\pi_1^2\pi_2^2\pi_3^2\ \sigma^2$ + 6.2% $\pi_1^2\pi_2^2\pi_3^2\ (\sigma^*)^2$		58.1% $\pi_1^2\pi_2^2\pi_3^2(\sigma^*)^{2e}$ + 7.5% $\pi_1^2\pi_2^2\pi_3^2\sigma^2$	
	^3B_u	66.1% $\pi_1^2\pi_2^2\pi_3^2\sigma^{*1}\sigma^1$	28.22	66.0% $\pi_1^2\pi_2^2\pi_3^2\sigma^{*1}\sigma^1$ + 2.2% $(8a_g)^1\pi_1^2\pi_2^2\pi_3^2\sigma^2\sigma^{*1}$	25.32[b]
meta (2,6)	$^1A_1$	54.0% $\pi_1^2\pi_2^2\pi_3^2\ \sigma^2$ + 12.8% $\pi_1^2\pi_2^2\pi_3^2\ (\sigma^*)^2$		57.5% $\pi_1^2\ \pi_2^2\pi_3^2\sigma^2$ + 10.8% $\pi_1^2\pi_2^2\pi_3^2\ (\sigma^*)^2$	
	$^3B_2$	64.0% $\pi_1^2\pi_2^2\pi_3^2\sigma^{*1}\sigma^1$	−1.40	57.0% $\pi_1^2\pi_2^2\pi_3^2\sigma^{*1}\sigma^1$ + 6.8% $(10a_1)^1\pi_1^2\pi_2^2\pi_3^2\sigma^2\sigma^{*1}$	−6.04[b]

[a]All absolute energies are reported in the Supporting Information in Table S7. [b]Intruder state has been added to the reference space at the MR-AQCC level. Details are included in the Computational Methods.

the geometrical distortion seen in the *ortho* (2,3) isomer C_2-C_3 bond but to a lesser extent. As a result of the C_{2h} molecular symmetry, there are shortened bonds indicative of bonding interactions on both sides of the molecule between N_1-C_2 and N_4-C_5. The $C_2-N_1-C_6$ angle is larger by 7.9° while the $N_1-C_6-C_5$ angle is smaller by 8.9°. In the triplet state, the N_1-C_2 shortening persists (0.05 Å) while the $N_1-C_2-C_3$ angle is 5.4° larger than in fully saturated pyrazine. The $C_6-N_1-C_2$ and $C_5-C_6-N_1$ are 2.9 and 2.6° smaller than the saturated bond angles, respectively. Other than these differences, the geometries in the *para* (2,5) triplet isomer are similar to fully saturated pyrazine.

There is little change in the bond lengths in the *meta* (2,6) isomer in either the triplet or singlet states relative to saturated pyrazine. The angles in the triplet are also very similar, differing by at most 1.9 degrees. However, there is a significant change (16.4 degrees) in the singlet state $C_2-N_1-C_6$ angle. Cross ring bonding interaction between the two dehydrocarbons is the cause of this ring pinching and a sign of through-space coupling between the radical electrons.[48] This interaction is emphasized in the MC-PDFT geometry where the ring is bicyclic and the C_2-C_6 bond is 1.53 Å.

Singlet−Triplet Energetic Gaps. The dominant configuration occupations and adiabatic gaps of all isomers using a CAS (8,8) active space are shown in Table 2. Vertical excitation gaps for the CASSCF (8,8), MR-CISD (8,8), and MR-AQCC (8,8) calculations are shown in Table 3. For the *ortho* (2,3) and *meta* (2,6) isomers, the singlet is the ground state with all methods except for the MR-AQCC (8,8) method. In *ortho* (2,3), MR-AQCC (8,8) predicts the triplet state to be lower in energy by 0.89 kcal/mol and in the *meta* (2,6) isomer it predicts an adiabatic gap of −6.04 kcal/mol with the triplet lying lowest. In the *para* (2,5) isomer, the gap is the largest (25.32 kcal/mol (AQCC)) with the singlet state as the ground state at each level of theory.

The singlet states of each isomer have two dominant configurations and contain three doubly occupied π orbitals and either a doubly occupied σ or σ^* orbital. The configuration containing a doubly occupied in-phase σ-orbital had the highest weight in each isomer (57% *ortho* (2,3); 58% *para* (2,5); 58% *meta* (2,6)). The configuration containing a doubly occupied antisymmetric σ^* orbital had the second highest weight (8.3% *ortho* (2,3); 7.5% *para* (2,5); 11% *meta* (2,6)).

At the CAS (8,8) level, each isomer has two dominant configurations in the triplet state. The first and most dominant configuration (59% in *ortho* (2,3); 66% in *para* (2,5); 57% in *meta* (2,6)) has the π-orbitals doubly occupied and an unpaired electron in each of the σ and σ^* orbitals. The second most significant configuration has doubly occupied π and σ orbitals and an unpaired electron in the σ^* orbital and in a DOCC orbital ($9a_1$ for *ortho* (2,3); $8a_g$ for *para* (2,5); $10a_1$ for *meta* (2,6)); these N-based orbitals are shown in Table 1B). The exclusion of these intruder state configurations in the CAS may account for the large difference between the MR-CISD (8,8) and the MR-CISD+Q (8,8) energies in the *para* (2,5) isomer and favoring of the triplet ground state for *ortho* (2,3) and *meta* (2,6) by MR-AQCC. MR-AQCC (12,10) single-point calculations on the MR-AQCC (8,8)/cc-pVTZ geometries were performed to investigate the importance of these orbitals in the active space (*vide infra*).

Expanding the Active Space to Include Lone Pair Electrons on Nitrogen Atoms. To determine the effect of including nitrogen atom lone pair electrons/orbitals in the active space, we performed MR-AQCC (12,10)/cc-pVTZ single-point calculations on MR-AQCC (8,8)/cc-pVTZ geometries. The energies and dominant configurations are compared with the MR-AQCC (8,8)/cc-pVTZ results in Table 4. From this, we see that the expansion of the active space results in singlet ground states for the ortho (2,3) and *para* (2,5) isomers with ΔE(ST) values of 1.78 and 28.22 kcal/mol, respectively and a triplet ground state in the *meta* (2,6) isomer with a ΔE(ST) of −1.40 kcal/mol. We also see that expanding the active space to include the nitrogen lone pair

DOI: 10.1021/acs.jpca.8b12440
J. Phys. Chem. A XXXX, XXX, XXX−XXX

orbitals results in triplet states dominated by one configuration, thereby eliminating the intruder states and supporting the hypothesis that CAS (8,8) was an insufficient active space to accurately describe these heteroaromatic diradical isomers.

Destabilization of the singlet state in the *meta* (2,6) isomer may stem from an unfavorable three-center−four-electron antibonding character of the $11a_1$ σ orbital (Table 1). In the 2,6-pyridine singlet isomer, Debbert et al.[49] found that the singlet state is destabilized because the antibonding orbital associated with the interaction of the nitrogen lone pair with the dehydrocarbons is comparable in energy to the σ^* orbital. A similar antibonding character is found in the σ orbital for *meta* (2,6) and may be the cause of the destabilization of the singlet state.

We also computed the adiabatic excitations using the computationally less costly MC-PDFT method with a (12,10) active space and the cc-pVTZ basis. It has been shown that MC-PDFT is comparable in accuracy to CASPT2 and has a computational cost comparable to CASSCF.[34] A comparison between CASPT2 and MC-PDFT is shown in Table 5.

Table 5. Adiabatic and Vertical Excitation Energies (kcal/mol) Calculated with MC-PDFT (12,10) and CASPT2 (12,10)

isomer	state	adiabatic MC-PDFT (12,10)[a]	vertical MC-PDFT (12,10)	adiabatic CASPT2 (12,10)[a]	vertical CASPT2 (12,10)
ortho (2,3)	$^1A_1$				
	$^3B_2$	4.13	25.54	1.53	20.31
para (2,5)	^1A_g				
	^3B_u	29.78	35.92	27.78	33.60
meta (2,6)	$^1A_1$				
	$^3B_2$	2.85	58.25	−0.87	19.55

[a]All absolute energies are reported in the Supporting Information in Table S7.

The CASPT2 method generally agrees with MC-PDFT. The biggest difference between the two methods is found in the vertical gap of the *meta* (2,6) isomer. In MC-PDFT, the geometry for the lowest lying singlet in *meta* (2,6) has a bond between the two diradical electrons. At the singlet geometry a triplet is a very unstable configuration as it corresponds to moving an electron into an orbital where the diradical lobes are out of phase. The difference in adiabatic gaps between MR-AQCC (12,10) and MC-PDFT (12,10) is at most 4.3 kcal/mol. This supports other work that has shown that MC-PDFT can describe diradical systems accurately.[50]

From these results we see that the *para* (2,5) isomer is the most promising as the basis of an antitumor warhead. Both the *ortho* (2,3) and *meta* (2,6) isomers have effectively degenerate singlet and triplet states. As the diradicals are more reactive in their triplet states, this suggests that a drug based on the *ortho* (2,3) or *meta* (2,6) scaffold might abstract hydrogen atoms indiscriminately. The *para* (2,5) isomer has a substantial adiabatic gap with a singlet ground state. Therefore, it may be possible to deliver a drug based on this diradical to an intended target before cyclization and tune its hydrogen-abstraction abilities.

Orbital Occupation Numbers, Effective Unpaired Electron Densities, and Spin Polarization. The MR-AQCC (12,10) natural orbital occupation numbers are shown graphically in Figure 3. In these plots one can see that in all

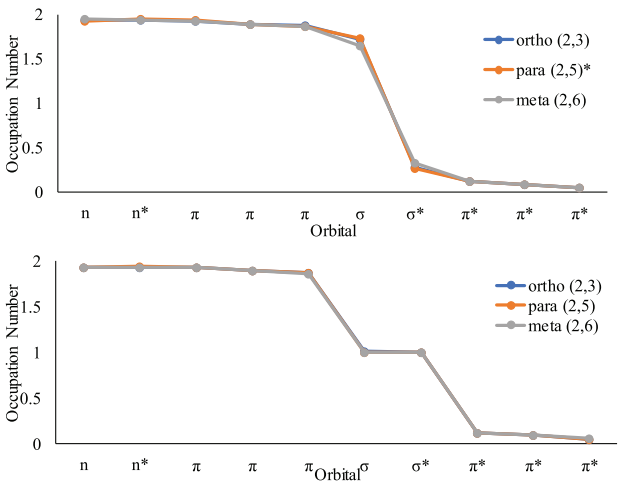

Figure 3. Occupation numbers of the MR-AQCC natural orbitals shown from highest occupation to lowest occupation. The ordering of the σ and σ^* orbitals is reversed in the *para* (2,5) isomer's singlet state. All calculations were performed with the CAS (12,10) active space. Top: singlet. Bottom: triplet.

isomers there is significant deviation from a true closed-shell singlet where all orbitals are doubly occupied. The σ/σ^* orbital occupations range from 1.60 to 1.75 and from 0.25 to 0.35 (the σ orbital lies lowest in the *ortho* (2,3) and *meta* (2,6) isomers while the σ^* lies lowest in the *para* (2,5) isomer). The π and π^* occupations are approximately 1.9 and 0.1, respectively. The *para* (2,5) isomer has the smallest deviation from a closed-shell singlet with σ and σ^* occupancies closest to 2.0 and 0.0. The occupancy of the triplet orbitals is similar in all isomers and generally follows the occupation of a true triplet. It should be noted that the antisymmetric σ^* orbital has a higher occupation number than the symmetric σ orbital in the *para* (2,5) isomer. This ordering is expected in this isomer because the diradicals are separated by three bonds in the ring. Hoffmann[48] has shown that separating diradicals in this way stabilizes the antisymmetric σ orbital in *para*-benzyne via through-bond coupling and in the case of *para* (2,5) the same stabilization is observed.

The unpaired electron density (UED) and the number of effectively unpaired electrons (N_U) provide a measure of the open-shell nature of a molecule. We determined the UED and N_U of the pyrazine isomers using the MR-AQCC (8,8)/cc-pVTZ wave function. The UED provides a visual and qualitative understanding of the degree of interaction between the radical electrons as well as the delocalization of the unpaired electrons whereas N_U provides a more quantitative comparison (Figure 4). As expected, for all isomers the singlet unpaired electron density is smaller than in the triplet. For each singlet isomer, the UED is localized on the dehydrocarbon atoms with some small amount of density on the nitrogen atoms. In each triplet isomer the UED is delocalized across the molecule while still having substantial density on the dehydrocarbons.

The magnitude of the N_U deviation of the singlet and triplet isomers from classical N_U values is notable−computing N_U using only σ and σ^* orbitals, the singlet N_U for *ortho* (2,3), *para* (2,5), and *meta* (2,6) is 0.78, 0.63, and 0.89 respectively,

DOI: 10.1021/acs.jpca.8b12440
J. Phys. Chem. A XXXX, XXX, XXX−XXX

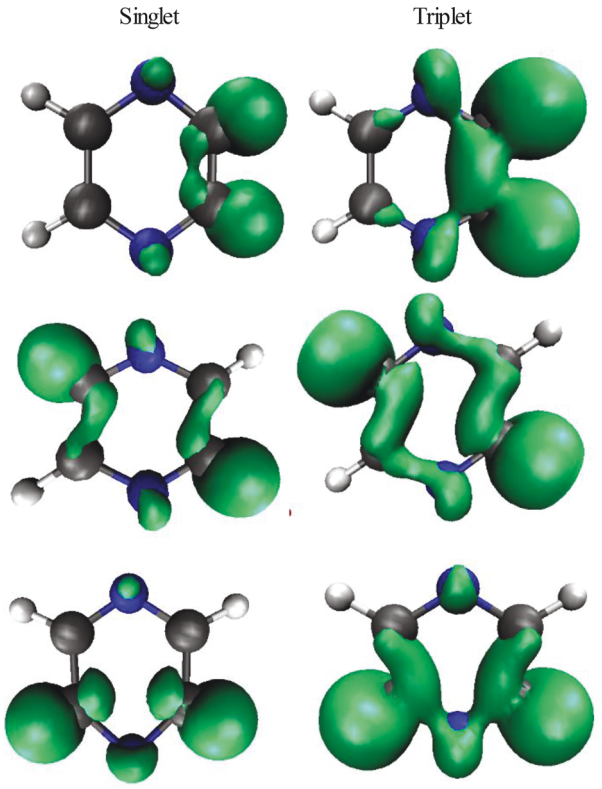

Figure 4. Unpaired electron density plots for the MR-AQCC (12,10)/cc-pVTZ calculation for both singlet and triplet states in each isomer (isovalue 0.007). Left: singlet. Right: triplet. Top: *ortho* (2,3). Middle: *para* (2,5). Bottom: *meta* (2,6).

suggesting a significant amount of coupling between the radical electrons (Table 6). Interestingly, the *para* (2,5) isomer shows

Table 6. MR-AQCC (12,10)/TZ N_U Values Computed Using Occupation Numbers of All CAS as Well as the σ and σ^* (HONO/LUNO) Orbitals

	ortho (2,3)		*para* (2,5)		*meta* (2,6)	
	singlet	triplet	singlet	triplet	singlet	triplet
N_U	0.71	2.24	0.66	2.24	0.88	2.25
N_U (HONO/LUNO)	0.48	2.00	0.42	2.00	0.64	2.00

a smaller N_U than the *ortho* (2,3) isomer; this is a bit surprising as in the *ortho* (2,3) isomer the radical electrons are proximate. However, this may be the result of coupling in the *para* (2,5) isomer between the unpaired electrons on the dehydrocarbons and the lone pairs on the nitrogen atoms as well as correlation between core electrons and imperfect pairing of bonding electrons. This also emphasizes the importance of through-bond coupling in the *para* (2,5) isomer. In the triplet the N_U values based on σ and σ^* are equal to 2.0 while the N_U values incorporating all CAS orbital occupations is slightly larger than 2.0 reflective of less than perfect pairing. Taken together, the UED, delocalization and N_U values indicate complex through-bond and through-space interactions in both isomers.

We also employed the intraatomic Hund's Rule to understand spin polarization and the electronic structure of each isomer including the interaction between the two unpaired electrons (Figure 5).[16] Bonding electrons are more stable when spin-paired and electrons on the same atom are more stable when arranged spin-parallel. In the *ortho* (2,3) and

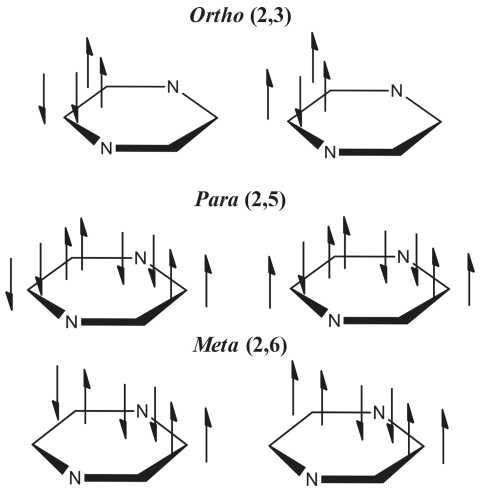

Figure 5. Spin polarization effects on the diradical carbons utilizing the intraatomic Hund's rule. Arrows on the bond represent bonding electrons and arrows outside of the ring represent the radical electrons. Bonding electrons are spin-paired. Right: singlet. Left: triplet.

para (2,5) isomers, the spin polarization rules imply that if the electron at one dehydrocarbon has an α spin, then the electron at the other dehydrocarbon must have a β spin. This interaction creates stabilizing $\beta-\beta$ spin interactions in the singlet state between the radical electron and the sigma bonding electron and a destabilizing $\alpha-\beta$ interaction in the triplet state (Figure 5). These interactions likely contribute to the singlet states lying lower in energy than the triplet states. In the *meta* (2,6) isomer the spin polarization stabilizes the triplet state, possibly contributing to the near-degeneracy of the singlet and triplet states in that isomer.

Literature Comparison. Cioslowski et al. performed single reference calculations on many diradicals including the isomers of diradical pyrazine.[8] The method most comparable in rigor to the methods used in this work is the quadratic configuration interaction with single and double excitations (QCISD). At this level of theory the *ortho* (2,3) isomer was reported not to exist. A DFT-based study by Chen et al. using the B3LYP functional and the LANL2DZ basis set showed that the *ortho* (2,3) isomer exists as an intermediate and predicts the ground state to be the triplet state, in disagreement with our findings.[6] For the *para* (2,5) isomer, the ΔE(ST) splitting computed with QCISD is 8.7 kcal/mol. This is significantly lower than our MR-AQCC/TZ result of 28.22 kcal/mol (Table 4). For the *meta* (2,6) isomer, the QCISD result suggests near-degeneracy between the singlet and triplet states, in perhaps fortuitous agreement with our results. The DFT results are comparable to MR-CISD and MR-CISD+Q in this isomer. A comparison of these data with the MR results is shown in Table 7. Geometrical comparisons with all literature values can be found in Table S6 in the Supporting Information.

CONCLUSIONS

The isomers of diradical pyrazine are possible antitumor drugs and intermediates in certain synthesis reactions. Extended active spaces were utilized in this study including all π and π^* orbitals with the σ and σ^* radical lobes (8,8). To probe the influence of the heteroatom, we also employed a (12,10) active space that included the nitrogen atom lone pair electrons and orbitals. Multireference methods, including CASSCF, MR-

DOI: 10.1021/acs.jpca.8b12440
J. Phys. Chem. A XXXX, XXX, XXX−XXX

Table 7. Comparison of Single-Reference and Multiple-Reference Results for the Singlet−Triplet Adiabatic Gaps (kcal/mol) for *Ortho* (2,3), *Para* (2,5), and *Meta* (2,6) Isomers of Pyrazine[a]

	basis set	2,3	2,5	2,6
MRCISD (8,8)	cc-pVTZ	7.89	19.45	2.01
MR-CISD+Q (8,8)	cc-pVTZ	6.03	25.82	2.26
MR-AQCC (8,8)	cc-pVTZ	−0.89	25.32[c]	−6.04[c]
MR-AQCC (12,10)	cc-pVTZ	1.78	28.22	−1.40
QCISD[8]	cc-pVTZ	*d*	8.7	−0.2
QCISD[8b]	cc-pVTZ	*d*	26.9	4.4
MC-PDFT (12,10)	cc-pVTZ	4.13	29.78	2.85
CASPT2 (12,10)	cc-pVTZ	1.53	27.78	−0.86
B3LYP[6]	311+G(d)	−9.9		2.10

[a]The MR-AQCC (12,10) results are considered the benchmark results. [b]Including thermal corrections. [c]Intruder state has been added to the reference space at the MR-AQCC level. Details are in included in the Computational Methods. [d]Found not to exist.

CISD+Q, MR-AQCC, CASPT2, and MC-PDFT were used to determine the ground states of each isomer, as well as to benchmark the energetic singlet−triplet splittings. The larger active space including the lone pairs on nitrogen was necessary for the proper physical characterization of these isomers. The singlet state was found to be the ground state in the *ortho* (2,3) and *para* (2,5) isomers while the ground state for the *meta* (2,6) isomer is a triplet. The singlet−triplet splittings were small for *ortho* (2,3) and *meta* (2,6) isomers, +1.78 and −1.40 kcal/mol, respectively. The splittings for the para isomer were significantly larger at 28.22 kcal/mol. It is encouraging that MC-PDFT, a method alternative to CASPT2 with a significantly lower cost, gives adiabatic singlet−triplet splittings in agreement within a few kcal/mol with MR-AQCC, suggesting that MC-PDFT can be used more routinely in the future. The relatively poor and inconsistent agreement between our multireference results and previously reported single reference results suggests that a multireference approach is necessary for describing the diradical isomers of pyrazine. All the methods suggest that the *para* (2,5) isomer is the most promising candidate for use in antitumor warhead drug design due to the large adiabatic single−triplet gap.

■ ASSOCIATED CONTENT

Supporting Information

The Supporting Information is available free of charge on the ACS Publications website at DOI: 10.1021/acs.jpca.8b12440.

Absolute energies, orbital energies, adiabatic and vertical energetic gaps, raw energies, and geometries (PDF)

■ AUTHOR INFORMATION

Corresponding Author

*email: cparish@richmond.edu, phone (804) 484-1548.

ORCID

Thais Scott: 0000-0002-5746-5517
Reed Nieman: 0000-0003-3011-5223
Adam Luxon: 0000-0002-4674-1942
Boyi Zhang: 0000-0002-0190-3776
Hans Lischka: 0000-0002-5656-3975
Laura Gagliardi: 0000-0001-5227-1396
Carol A. Parish: 0000-0003-2878-3070

Notes

The authors declare no competing financial interest.

■ ACKNOWLEDGMENTS

This work was supported in part by the Department of Energy (Grant DE-SC0001093 (C.P.)) and the National Science Foundation (Grant CHE-1213271 and CHE-18800014 (C.P.) and Grant CHE-1213263 (H.L.)). C.P. acknowledges the Donors of the American Chemical Society Petroleum Research Fund. Computational resources were provided, in part, by the MERCURY supercomputer consortium under NSF grant CHE-1626238. This work was also supported in part (L.G.) by the National Science Foundation by grant no. CHE-1464536. T.S. acknowledges that this material is also based upon work supported by the National Science Foundation Graduate Research Fellowship Program under Grant No. CON-75851, project 00074041. Any opinions, findings, and conclusions or recommendations expressed in this material are those of the author(s) and do not necessarily reflect the views of the National Science Foundation. T.S. and B.Z. acknowledge support from the University of Richmond Arts and Sciences Undergraduate Research Committee. A.L. acknowledges support from the Arnold and Mabel Beckman Foundation through receipt of a Beckman Scholars award.

■ REFERENCES

(1) Konishi, M.; Ohkuma, H.; Matsumoto, K.; Tsundo, T.; Kamei, H.; Miyaki, T.; Oki, T.; Kawaguchi, H.; VanDuyne, G.; Clardy, J. Dynemicin A, a novel antibiotic with the anthraquinone and 1,5-diyn-3-ene subunit. *J. Antibiot.* **1989**, *42*, 1449−1452.

(2) Golik, J.; Dubay, G.; Groenewold, G.; Kawaguchi, H.; Konishi, M.; Krishnan, B.; Ohkuma, H.; Saitoh, K.; Doyle, T. W. Esperamicins, a novel class of potent antitumor antibiotics. 3. Structures of esperamicins A1, A2, and A1b. *J. Am. Chem. Soc.* **1987**, *109*, 3462−3464.

(3) Zein, N.; Sinha, A. M.; McGahren, W. J.; Ellestad, G. A. Calicheamicin gamma 1i: An antitumor antibiotic that cleaves double-stranded DNA site specifically. *Science* **1988**, *240*, 1198−1201.

(4) Abe, M. Diradicals. *Chem. Rev.* **2013**, *113*, 7011−7088.

(5) Denonne, F.; Seiler, P.; Diederich, F. Towards the synthesis of azoacetylenes. *Helv. Chim. Acta* **2003**, *86*, 3096−3117.

(6) Chen, H.; Jacobson, D. B.; Freiser, B. S. Generation, characterization, and reactivity of the transition metal-o-benzyne analog of pyrazine (Fe^{+}− 2, 3-didehydropyrazine) in the gas phase: An experimental and theoretical study. *Organometallics* **1999**, *18*, 1774−1785.

(7) Crow, W. D.; Solly, R. K. Reactions of excited molecules. I. A thermal four-centre migration in phenylhydrazones. *Aust. J. Chem.* **1966**, *19*, 2119−2126.

(8) Cioslowski, J.; Szarecka, A.; Moncrieff, D. Energetics, electronic structures and geometries of didehydroazines. *Mol. Phys.* **2003**, *101*, 839−858.

(9) Kraka, E.; Cremer, D. The para-didehydropyridine, para-didehydropyridinium, and related biradicals—a contribution to the chemistry of enediyne antitumor drugs. *J. Comput. Chem.* **2001**, *22*, 216−229.

(10) Slipchenko, L. V.; Krylov, A. I. Singlet-triplet gaps in diradicals by the spin-flip approach: A benchmark study. *J. Chem. Phys.* **2002**, *117*, 4694−4708.

(11) Wang, E. B.; Parish, C. A.; Lischka, H. An extended multireference study of the electronic states of para-benzyne. *J. Chem. Phys.* **2008**, *129*, No. 044306.

(12) Clark, A. E.; Davidson, E. R.; Zaleski, J. M. UDFT and MCSCF descriptions of the photochemical bergman cyclization of enediynes. *J. Am. Chem. Soc.* **2001**, *123*, 2650−2657.

DOI: 10.1021/acs.jpca.8b12440
J. Phys. Chem. A XXXX, XXX, XXX−XXX

(13) Evangelista, F. A.; Allen, W. D.; Schaefer, H. F., III Coupling term derivation and general implementation of state-specific multi-reference coupled cluster theories. *J. Chem. Phys.* **2007**, *127*, No. 024102.
(14) Kraka, E.; Cremer, D. Ortho-, meta-, and para-benzyne. A comparative CCSD(T) investigation. *Chem. Phys. Lett.* **1993**, *216*, 333−340.
(15) Schreiber, M.; Silva-Junior, M. R.; Sauer, S. P.; Thiel, W. Benchmarks for electronically excited states: CASPT2, CC2, CCSD, and CC3. *J. Chem. Phys.* **2008**, *128*, 134110.
(16) Crawford, T. D.; Kraka, E.; Stanton, J. F.; Cremer, D. Problematic p-benzyne: Orbital instabilities, biradical character, and broken symmetry. *J. Chem. Phys.* **2001**, *114*, 10638−10650.
(17) Evangelista, F. A.; Hanauer, M.; Köhn, A.; Gauss, J. A sequential transformation approach to the internally contracted multireference coupled cluster method. *J. Chem. Phys.* **2012**, *136*, 204108.
(18) Greenman, L.; Mazziotti, D. A. Highly multireferenced arynes studied with large active spaces using two-electron reduced density matrices. *J. Chem. Phys.* **2009**, *130*, 184101.
(19) Horn, S.; Plasser, F.; Müller, T.; Libisch, F.; Burgdörfer, J.; Lischka, H. A comparison of singlet and triplet states for one-and two-dimensional graphene nanoribbons using multireference theory. *Theor. Chem. Acc.* **2014**, *133*, 1511−1518.
(20) Das, A.; Müller, T.; Plasser, F.; Lischka, H. Polyradical character of triangular non-kekulé structures, zethrenes, p-quinodimethane-linked bisphenalenyl, and the clar goblet in comparison: An extended multireference study. *J. Phys. Chem. A* **2016**, *120*, 1625−1636.
(21) Pinheiro, M.; Das, A.; Aquino, A. J.; Lischka, H.; Machado, F. B. C. Interplay between aromaticity and radicaloid character in nitrogen-doped oligoacenes revealed by high-level multireference methods. *J. Phys. Chem. A* **2018**, *122*, 9464.
(22) Das, A.; Pinheiro, M., Jr; Machado, F. B.; Aquino, A. J.; Lischka, H. Tuning the biradicaloid nature of polycyclic aromatic hydrocarbons: The effect of graphitic nitrogen doping in zethrenes. *ChemPhysChem* **2018**, *19*, 2492−2499.
(23) Ghosh, S.; Cramer, C. J.; Truhlar, D. G.; Gagliardi, L. Generalized-active-space pair-density functional theory: An efficient method to study large, strongly correlated, conjugated systems. *Chem. Sci.* **2017**, *8*, 2741−2750.
(24) Frisch, M. J.; Trucks, G. W.; Schlegel, H. B.; Scuseria, G. E.; Robb, M. A.; Cheeseman, J. R.; Scalmani, G.; Barone, V.; Petersson, G. A.; Nakatsuji, H.; et al. *Gaussian 16* rev. B.01; Wallingford, CT, 2016.
(25) Dunning, T. H., Jr Gaussian basis sets for use in correlated molecular calculations. I. The atoms boron through neon and hydrogen. *J. Chem. Phys.* **1989**, *90*, 1007−1023.
(26) Kendall, R. A.; Dunning, T. H., Jr; Harrison, R. J. Electron affinities of the first-row atoms revisited. Systematic basis sets and wave functions. *J. Chem. Phys.* **1992**, *96*, 6796−6806.
(27) Roos, B. The complete active space self-consistent field method and its applications in electronic structure calculations. *Adv. Chem. Phys.* **2007**, 399.
(28) Szalay, P. G.; Müller, T.; Gidofalvi, G.; Lischka, H.; Shepard, R. Multiconfiguration self-consistent field and multireference configuration interaction methods and applications. *Chem. Rev.* **2012**, *112*, 108−181.
(29) Lischka, H.; Nachtigallová, D.; Aquino, A. J. A.; Szalay, P. G.; Plasser, F.; Machado, F. B. C.; Barbatti, M. Multireference approaches for excited states of molecules. *Chem. Rev.* **2018**, *118*, 7293−7361.
(30) Lischka, H.; Shepard, R.; Pitzer, R. M.; Shavitt, I.; Dallos, M.; Müller, T.; Szalay, P. G.; Seth, M.; Kedziora, G. S.; Yabushita, S.; Zhang, Z. High-level multireference methods in the quantum-chemistry program system columbus: Analytic MR-CISD and MR-AQCC gradients and MR-AQCC-LRT for excited states, GUGA spin−orbit CI and parallel CI density. *Phys. Chem. Chem. Phys.* **2001**, *3*, 664−673.
(31) Malrieu, J. P.; Daudey, J. P.; Caballol, R. Multireference self-consistent size-consistent singles and doubles configuration interaction for ground and excited states. *J. Chem. Phys.* **1994**, *101*, 8908−8921.
(32) Szalay, P. G.; Bartlett, R. J. Multi-reference averaged quadratic coupled-cluster method: A size-extensive modification of multi-reference CI. *Chem. Phys. Lett.* **1993**, *214*, 481−488.
(33) Li Manni, G.; Carlson, R. K.; Luo, S.; Ma, D.; Olsen, J.; Truhlar, D. G.; Gagliardi, L. Multiconfiguration pair-density functional theory. *J. Chem. Theory Comput.* **2014**, *10*, 3669−3680.
(34) Gagliardi, L.; Truhlar, D. G.; Li Manni, G.; Carlson, R. K.; Hoyer, C. E.; Bao, J. L. Multiconfiguration pair-density functional theory: A new way to treat strongly correlated systems. *Acc. Chem. Res.* **2017**, *50*, 66−73.
(35) Sand, A. M.; Hoyer, C. E.; Sharkas, K.; Kidder, K. M.; Lindh, R.; Truhlar, D. G.; Gagliardi, L. Analytic gradients for complete active space pair-density functional theory. *J. Chem. Theory Comput.* **2018**, *14*, 126−138.
(36) Aquilante, F.; Autschbach, J.; Carlson, R. K.; Chibotaru, L. F.; Delcey, M. G.; De Vico, L.; Galván, I. F.; Ferré, N.; Frutos, L. M.; Gagliardi, L.; et al. Molcas 8: New capabilities for multiconfigurational quantum chemical calculations across the periodic table. *J. Comput. Chem.* **2016**, *37*, 506−541.
(37) Lischka, H.; Shepard, R.; Shavitt, I.; Pitzer, R.; Dallos, M.; Muller, T.; Szalay, P.; Brown, F. B.; Ahlrichs, R.; Bohm, H. J.; et al. *Columbus, an ab initio electronic structure program*, release 7.0; 2017; https://www.univie.ac.at/columbus/.
(38) Dachsel, H.; Lischka, H.; Shepard, R.; Nieplocha, J.; Harrison, R. J. A massively parallel multireference configuration interaction program: The parallel COLUMBUS program. *J. Comput. Chem.* **1997**, *18*, 430−448.
(39) Szalay, P. G.; Müller, T.; Lischka, H. Excitation energies and transition moments by the multireference averaged quadratic coupled cluster (MR-AQCC) method. *Phys. Chem. Chem. Phys.* **2000**, *2*, 2067−2073.
(40) Lischka, H.; Müller, T.; Szalay, P. G.; Shavitt, I.; Pitzer, R. M.; Shepard, R. COLUMBUS—a program system for advanced multi-reference theory calculations. *Wiley Interdiscip. Rev. Comput. Mol. Sci.* **2011**, *1*, 191−199.
(41) Head-Gordon, M. Characterizing unpaired electrons from the one-particle density matrix. *Chem. Phys. Lett.* **2003**, *372*, 508−511.
(42) Schaftenaar, G.; Vlieg, E.; Vriend, G. Molden 2.0: Quantum chemistry meets proteins. *J. Comput.-Aided Mol. Des.* **2017**, *31*, 789−800.
(43) *Jmol: An open-source java viewer for chemical structures in 3D*. http://www.Jmol.Org/.
(44) Humphrey, W.; Dalke, A.; Schulten, K. VMD: Visual Molecular Dynamics. *J. Mol. Graphics* **1996**, *14*, 33−38.
(45) Bormans, B. J. M.; De With, G.; Mijlhoff, F. C. The molecular structure of pyrazine as determined from gas-phase electron diffraction data. *J. Mol. Struct.* **1977**, *42*, 121−128.
(46) Budzák, S.; Scalmani, G.; Jacquemin, D. Accurate excited-state geometries: A CASPT2 and coupled-cluster reference database for small molecules. *J. Chem. Theory Comput.* **2017**, *13*, 6237−6252.
(47) Dkhar, P. G. S.; Lyngdoh, R. H. D. Generation, structure and reactivity of arynes: A theoretical study. *Proc. - Indian Acad. Sci., Chem. Sci.* **2000**, *112*, 97−108.
(48) Hoffmann, R. Interaction of orbitals through space and through bonds. *Acc. Chem. Res.* **1971**, *4*, 1−9.
(49) Debbert, S. L.; Cramer, C. J. Systematic comparison of the benzynes, pyridynes, and pyridynium cations and characterization of the bergman cyclization of z-but-1-en-3-yn-1-yl isonitrile to the meta diradical 2, 4-pyridyne. *Int. J. Mass Spectrom.* **2000**, *201*, 1−15.
(50) Stoneburner, S. J.; Truhlar, D. G.; Gagliardi, L. Mc-PDFT can calculate singlet−triplet splittings of organic diradicals. *J. Chem. Phys.* **2018**, *148*, No. 064108.

DOI: 10.1021/acs.jpca.8b12440
J. Phys. Chem. A XXXX, XXX, XXX−XXX